Applied Surface Science 599 (2022) 153901

Contents lists available at ScienceDirect

Applied Surface Science

journal homepage: www.elsevier.com/locate/apsusc

Full Length Article

Band alignment of orthorhombic Ga_2O_3 with GaN and AlN semiconductors

Shibin Krishna *, Yi Lu, Che-Hao Liao, Vishal Khandelwal, Xiaohang Li *

King Abdullah University of Science and Technology (KAUST), Advanced Semiconductor Laboratory, Thuwal 23955, Saudi Arabia

ARTICLE INFO

Keywords:
Band alignment
Orthorhombic Ga_2O_3
GaN
AlN

ABSTRACT

Ga_2O_3 semiconductors have attracted tremendous research interests because of their fascinating material properties for future-generation energy, electronic, and optoelectronic applications. In the present study, we have performed the epitaxial growth of tin-doped Ga_2O_3 on sapphire, GaN, and AlN templates by the pulsed laser deposition technique. The initial characterizations show a two-dimensional mode of single-crystalline orthorhombic Ga_2O_3 (κ-Ga_2O_3) growth on these substrates with smooth surface morphology. Integrating κ-Ga_2O_3 with nitride semiconductors is interesting since both these materials possess polarization, which could induce 2-dimensional carrier gas (2DCG) at the interface. X-ray photoelectron spectroscopy studies reveal that both κ-Ga_2O_3/GaN and κ-Ga_2O_3/AlN heterostructure form a type-I band structure where the conduction band offset (CBO) was calculated to be 1.38 eV and 1.04 eV, respectively. This unique band alignment with high CBO could lead to the development of efficient power devices.

1. Introduction

Power device technology plays a central role in numerous crucial applications, including electric vehicles, solar farms, 5G/6G, and data centers [1–3]. GaN and AlN are promising wide bandgap (WBG) semiconductors that lead to power devices which operate with considerably higher voltage and efficiency than conventional silicon with smaller bandgap and breakdown field [4]. With decades of development, nitride-based power devices have entered wide market adoption. However, despite that the Ga_2O_3 ultra-wide bandgap (UWBG) semiconductor possesses an even greater Baliga figure of merit [5], the research and commercialization of Ga_2O_3-based power devices are still at the relatively early stage due to some serious issues such as a lack of effective p-doping techniques and poor thermal conductivity [4].

There are mainly different polymorphs for Ga_2O_3, comprising corundum (α), monoclinic (β), defective spinel (γ), cubic (δ), hexagonal (ε), and orthorhombic (κ) phase [6]. One of the polymorphs of Ga_2O_3, β-Ga_2O_3, has been well explored concerning the growth, material properties, and devices because of its high thermal stability [7–9]. However, the other polymorph of Ga_2O_3 are still behind as most of them are in a metastable state and change to a stable β phase at higher temperatures (>500 °C)[10]. Interestingly, in the orthorhombic phase, one of the metastable phases of Ga_2O_3, represented as κ-Ga_2O_3, shows spontaneous polarization [11,12] and high-temperature stability till 1000°C[13]. Lately, κ-Ga_2O_3 has captivated huge research attention due to the predicted high value of its spontaneous polarization i.e., 0.23 C/m^2 [14,15]. Therefore, this promising property can effectively control the two-dimensional carrier gas (2DCG) at the interfaces between κ-Ga_2O_3 and other suitable semiconductors without any chemical impurity doping. Hence, integrating high polarisation semiconductors such as nitride (spontaneous polarization of AlN = 1.33 C/m; GaN = 1.33 C/m) [16] with κ-Ga_2O_3 semiconductors can lead to huge polarization difference which opens a prospect to control the interfacial conductivity similar to an AlGaN/GaN heterostructure [17,18]. Furthermore, as compared to nitride semiconductors, the κ-Ga_2O_3 phase could show not only the polarization but also the ferroelectric property. This suggests that the spontaneous polarization of κ-Ga_2O_3 could be changed by applying an external electric field [19].

Therefore, integrating existing nitride technology with κ-Ga_2O_3 semiconductors can provide a favorable platform for exploring emerging phenomena, which motivates new concepts for fundamental physics and applied research. Moreover, this combination can effectively alleviate the thermal issue of κ-Ga_2O_3. Thereby, fundamental properties of κ-Ga_2O_3 based heterostructures, such as the energy band diagram, band alignment, built-in interface potential, and polarity discontinuity, are crucial for the tuning of polar oxide interfaces toward advanced devices [20]. We have previously studied the band alignment of β-Ga_2O_3 and AlN, and a type-II heterostructure has been witnessed [21]. In this work, the study of valence and conduction band offsets (VBO and CBO) of κ-Ga_2O_3/GaN and κ-Ga_2O_3/AlN heterojunctions have been calculated

* Corresponding author.
E-mail addresses: shibin.chandroth@kaust.edu.sa (S. Krishna), xiaohang.li@kaust.edu.sa (X. Li).

https://doi.org/10.1016/j.apsusc.2022.153901
Received 13 April 2022; Received in revised form 25 May 2022; Accepted 4 June 2022
Available online 11 June 2022

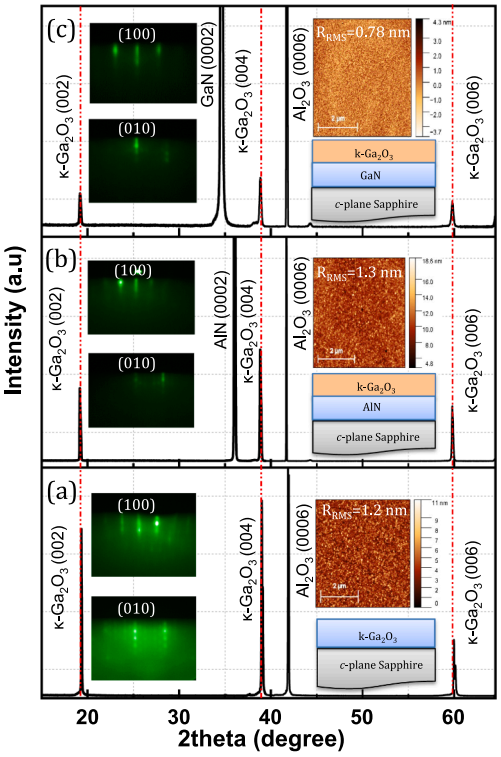

Fig. 1. XRD 2theta-omega scan profiles of κ-Ga_2O_3 layers grown on (a) c-plane Sapphire (0001), (b) AlN (0001), and (c) GaN (0001). The left inset represents the RHEED images along (1 0 0) and (0 1 0) azimuthal planes where a two-dimensional film growth was witnessed. The right insets show the corresponding AFM image and schematic of the growth structure.

experimentally and type-I band alignments for both combinations are confirmed. The band offset of κ-Ga_2O_3/nitride heterostructure is extremely important because it ascertains the energy barriers in electron and hole transport for the efficient working of electronic and optical devices.

2. Experimental section

In this work, we perform the pulsed laser deposition (PLD) technique for the growth of κ-Ga_2O_3 on sapphire, GaN, and AlN templates. The 3 μm epitaxial GaN and AlN growths were carried out in a Taiyo Nippon Sanso SR-4000HT horizontal Metal Organic Chemical Vapor Deposition (MOCVD) system on a c-plane sapphire substrate. Trimethylaluminum (TMA), trimethylgallium (TMG), and ammonia (NH_3) were used as precursors with nitrogen (N_2) as the carrier gas. The substrate growth temperature is 1340°C and 1150°C while V/III ratio is 742 and 2423 for AlN and GaN growth respectively. Prior to the PLD deposition, the sapphire substrate, MOCVD grown GaN and AlN templates were cleaned ultrasonically with acetone (5 min) followed by isopropyl alcohol (5 min) and then rinsed with deionized water. The tin doped (1.5 wt%) Ga_2O_3 target was irradiated using a KrF excimer laser (λ = 248 nm) at 100 mJ (on the target) for 15,000 pulses at a frequency of 2 Hz for bulk samples with a thickness of 360 nm. Further, 3 nm thick κ-Ga_2O_3 was grown on GaN and AlN template for high-resolution X-ray photoemission spectroscopy (HR-XPS) heterointerface analysis. The growth was performed at a substrate temperature of 650°C without the presence of oxygen partial pressure (chamber vacuum: $6x10^{-7}$ Torr). The crystal quality of the PLD grown κ-Ga_2O_3 on the various substrates has been analyzed by X-Ray diffractometer (XRD) and high-resolution scanning transmission electron microscopy (HR-STEM).

3. Results and discussion

Fig. 1 shows the XRD 2theta-omega scan profiles of κ-Ga_2O_3 layers directly grown on (a) c-plane Sapphire (0001), (b) AlN (0001), and (c) GaN (0001) substrates. κ-Ga_2O_3 films were grown along (0 0 1) direction for all the substrates where the 2theta angle positioned at 19.15°, 38.80°, and 59.75° represents the (0 0 2), (0 0 4) and (0 0 6) plane of diffraction of κ-Ga_2O_3. The 2theta scan is also represented in logarithmic scale to see each reflection in detail (supplementary information S1). The sharp and intense X-Ray diffraction peaks of κ-Ga_2O_3 divulge the single crystalline hetero-epitaxial growth on sapphire, GaN, and AlN templates. Further, 2theta positions perceived at 34.5° and 36° belong to GaN and AlN, respectively. All the XRD peak positions are calibrated with a sapphire substrate peak at 41.6°. To confirm the orthorhombic phase of Ga_2O_3, ϕ scan for a 2θ value of 33.05° and a χ value of 54.67° is performed (supplementary information S1). At this particular angle, only (1 2 2) reflex of the orthorhombic lattice can be observed [22,23]. The 12 peaks correspond to three rotation domains of orthorhombic κ-Ga_2O_3 which are not overlapping in direction with the ones of other domains. The epitaxial relationship between κ-Ga_2O_3 with sapphire is represented as ⟨0 0 1⟩ κ-Ga_2O_3 || <0001 > Al_2O_3, ⟨0 1 0⟩ κ-Ga_2O_3 || <11–20 > Al_2O_3 and ⟨1 0 0⟩ κ-Ga_2O_3 || <1–100 > Al_2O_3 [24,25].

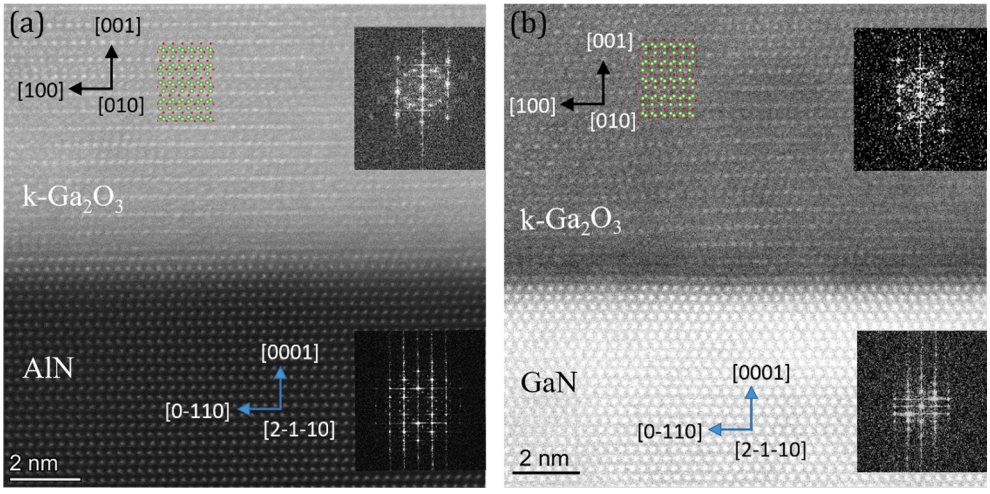

Fig. 2. HAADF-STEM images of the cross-sectional view of (a) κ-Ga_2O_3/AlN interface and (b) κ-Ga_2O_3/GaN interface, respectively. Both images are taken along the [11–20] zone axis of AlN and GaN, as shown in the inset of the corresponding FFT (a) and (b). A crystal model of κ-Ga_2O_3 along its [0 1 0] zone axis is overlayed on the as-grown thin film.

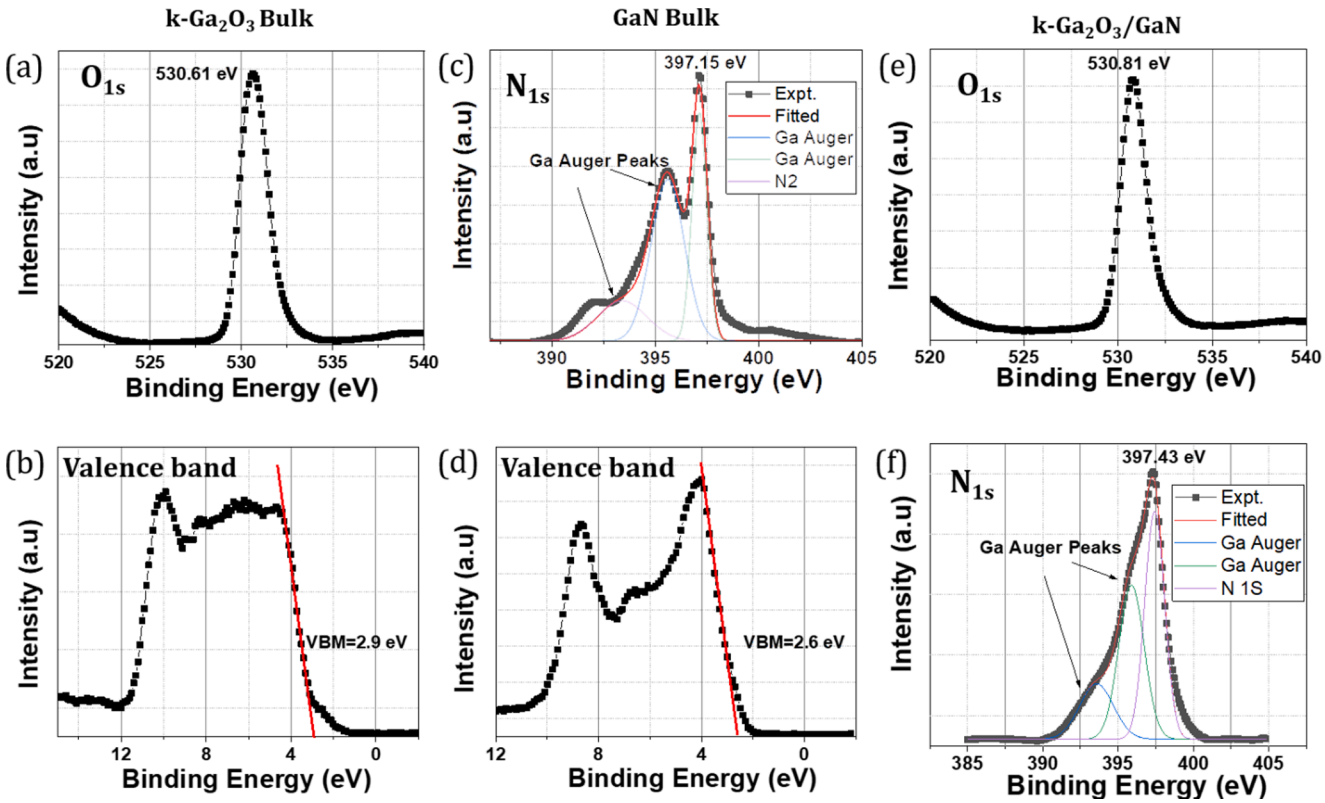

Fig. 3. XPS core level spectra of (a) O_{1s} and (b) valence band spectra of the bulk κ-Ga_2O_3; core level spectra of (c) N_{1s} and (d) valence band spectra of the bulk GaN; core level spectra of (e) O_{1s} and (f) N_{1s} of the κ-Ga_2O_3/GaN heterostructure.

The structural properties were further cross-examined by Reflection High Energy Electron Diffraction (RHEED) and Atomic Force Microscopy (AFM). The inset of Fig. 1 represents the AFM and RHEED pattern of κ-Ga_2O_3 grown on various substrates. The bottom right inset of Fig. 1 exemplifies the corresponding growth structure schematics. A very smooth and uniform surface morphology was witnessed in the AFM images shown in top right inset for all the samples. The Root Mean Square (RMS) roughness values are 1.2 nm, 1.3 nm and 0.78 nm, respectively for the sample grown on sapphire, AlN, and GaN. The left inset represents the RHEED images along (1 0 0) and (0 1 0) azimuthal planes. A prominent streaky patterns along with 6x6 reconstruction (along (0 1 0)) were observed on κ-Ga_2O_3 grown on sapphire, AlN and GaN templates. The streaky pattern in both azimuthal images confirms the two-dimensional growth with highly single crystalline nature.

Further, the heterostructure interface quality was scrutinized by STEM. The cross-sectional STEM images of the κ-Ga_2O_3/AlN and κ-Ga_2O_3/GaN heterostructure are represented in the supplementary information S2. It exhibits a columnar growth of the material along (0 0 1) zone axis. Fig. 2 a) and 2b) shows the cross sectional high angle annular dark-field (HAADF) image of κ-Ga_2O_3/AlN and κ-Ga_2O_3/GaN heterostructure, respectively. It exemplifies a sharp interface between the heterostructure and aligned, well-ordered crystal lattice of κ-Ga_2O_3, AlN and GaN. Moreover, HR-STEM observations reveal that as-grown κ-Ga_2O_3 layer has a high crystal-quality with clear and regular atomic arrangement. The inset image represents the corresponding Fast Fourier transform (FFT) of each layer which possesses the hexagonal wurtzite features of AlN and GaN template while an orthorhombic crystal structure feature of κ-Ga_2O_3 [26]. An orthorhombic crystal model of κ-Ga_2O_3 along its [0 1 0] zone axis overlayed on the as-grown thin film is in very good match with our TEM observation, which indicates that the as-grown thin film is κ-Ga_2O_3. Therefore, their epitaxial relationships are ⟨0 1 0⟩ κ-Ga_2O_3 || <11–20 > AlN and ⟨0 1 0⟩ κ-Ga_2O_3 || <11–20 > GaN, respectively. No rotation domains of κ-Ga_2O_3 are observed in this experiment. Furthermore, the atomic sharp interface between κ-Ga_2O_3 and the corresponding substrate indicates that there is no transition layer during the thin film growth [23].

Band alignment of κ-Ga_2O_3/GaN and κ-Ga_2O_3/AlN heterostructures were measured by HR-XPS. The HR-XPS measurements have been performed using a Kratos Axis Ultra DLD spectrometer equipped with a monochromatic $Al_{K\alpha}$ X-ray source (hγ = 1486.6 eV) operating at 150 W, a multi-channel plate, and a delay line detector under a vacuum of ~ 10^{-9} Torr. The binding energy of the C_{1s} peak (284.8 eV) was used as a standard reference. The valence band offset, VBO (ΔE_v) of κ-Ga_2O_3, and GaN can be calculated from the following formula:

$$\Delta E_V = (E_{O1s}^{k-Ga2O3} - E_{VBM}^{k-Ga2O3}) - (E_{N1s}^{GaN} - E_{VBM}^{GaN}) - (E_{O1s}^{k-Ga2O3/GaN} - E_{N1s}^{k-Ga2O3/GaN}) \quad (1)$$

$E_{O1s}^{k-Ga2O3}$ and E_{N1s}^{GaN} represent the O_{1s} and N_{1s} binding energy position of bulk κ-Ga_2O_3 and GaN film, while E_{VBM} denotes the valence band maximum (VBM) position of respective samples. The core level (CL) and valence band (VB) spectra of the bulk κ-Ga_2O_3 film are shown in Fig. 3 (a) and Fig. 3 (b), respectively. Fig. 3 (a) illustrates the O_{1s} CL spectrum acquired from the κ-Ga_2O_3 layer which manifests a single peak at 530.61 eV, corresponding to the Ga-O bond. Fig. 3(b) represents the valence band spectrum where VBM is estimated by linearly extrapolating the leading edge to the baseline of the respective valence band photoelectron spectrum. The VBM of the κ-Ga_2O_3 is measured to be 2.9 eV. Thereby, the separation between the CL energies of O_{1s} and VBM [$\Delta E = (E_{O1s}^{k-Ga2O3} - E_{VBM}^{k-Ga2O3})$] is 527.71 eV.

To determine the term in the second bracket in Eq. (1), XPS spectra of the bulk GaN were acquired. Fig. 3 (c) and 3 (d) represent the N_{1s} CL and VB spectra of GaN. The N_{1s} spectrum is deconvoluted into three peaks to exactly calculate the binding energy position of the Ga-N bond. The first two peaks positioned at 383.4 eV and 395.55 eV correspond to Ga-Auger peaks. However, the deconvoluted third peak corresponds to the Ga-N

Table 1
Fitting parameters used for VBO calculation of κ-Ga_2O_3/GaN.

Sample	State	Binding energy (eV)	Bonding	FWHM (eV)
κ-Ga_2O_3	O_{1s}	530.61	Ga-O	1.7
	VBM	2.9		
GaN	N_{1s}	397.15	Ga-N	1.2
	VBM	2.6		
κ-Ga_2O_3/GaN	O_{1s}	530.81	Ga-O	1.5
	N_{1s}	397.43	Ga-N	1.2

bond from the N_{1s} spectrum which is positioned at 397.15 eV. Therefore, the difference between the CL energies of N_{1s} and VBM [$\Delta E = (E_{N1s}^{GaN} - E_{VBM}^{GaN})$] is determined to be 394.55 eV. The details of the fitting parameters and binding energy positions are tabulated in Table 1. The last bracket term in Eq. (1) represents the CL separation between the O_{1s} and N_{1s} peaks from the XPS measurement of κ-Ga_2O_3/GaN heterostructure. Fig. 3(e) and 3(f) show the O_{1s} and N_{1s} CLs, which is originated from κ-Ga_2O_3/GaN heterostructure, respectively. Fig. 3(e) represents the single peak of O_{1s} positioned at 530.81 eV. Further, the N_{1s} CL spectrum of the heterostructure was deconvoluted to three peaks, and the peak corresponding to the Ga-N bond from the N_{1s} spectrum is positioned at 397.43 eV. Thereby, the energy difference between the CLs of $(E_{O1s}^{k-Ga2O3/GaN} - E_{N1s}^{k-Ga2O3/GaN})$ is 133.38 eV. Thus, the VBO is calculated to be − 0.22 ± 0.07 eV (the error value is calculated by considering the fitting error and discrepancy in the repeated measurements). The conduction band offset, CBO (ΔE_C) for κ-Ga_2O_3/GaN heterostructure is determined by substituting the VBO and electronic bandgap (E_g) values of κ-Ga_2O_3 and GaN in equation (2),

$$\Delta E_C = E_g^{k-Ga2O3} - E_g^{GaN} + \Delta E_v \quad (2)$$

$E_g^{k-Ga2O3}$ and E_g^{GaN} were measured from the transmittance tauc plot, and it is calculated to be 5.0 eV and 3.44 eV, respectively (supplementary information S3). Hence, the CBO is estimated to be 1.38 ± 0.07 eV. These experimentally determined parameters are assimilated into a band alignment diagram as represented in Fig. 5, which divulges that the κ- Ga_2O_3/GaN heterostructure forms a type-I band alignment. This peculiar band alignment with high CBO and huge polarization difference of the materials could form the two dimensional electron gas (2DEG) at the interface. The dependency of polarity (Ga and N-polar) on the band alignment of κ-Ga_2O_3/GaN will be an interesting study to be carried out in the future. Further, the band alignment of κ-Ga_2O_3 with AlN WBG semiconductor is depicted below,

The valence band offset of κ-Ga_2O_3 with AlN can be calculated from the following formula:

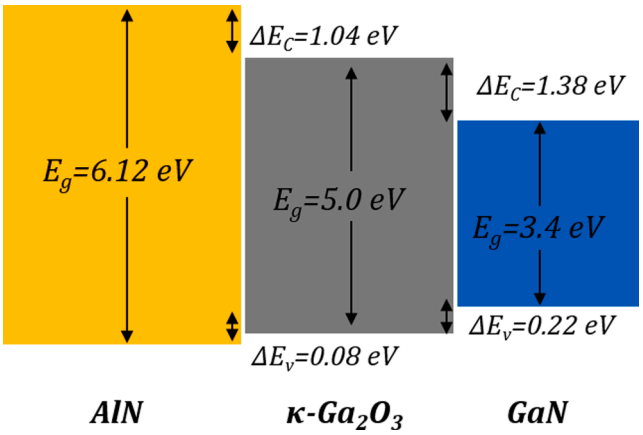

Fig. 5. The band alignment diagram of the κ-Ga_2O_3/GaN heterojunction, along with that of κ-Ga_2O_3/AlN.

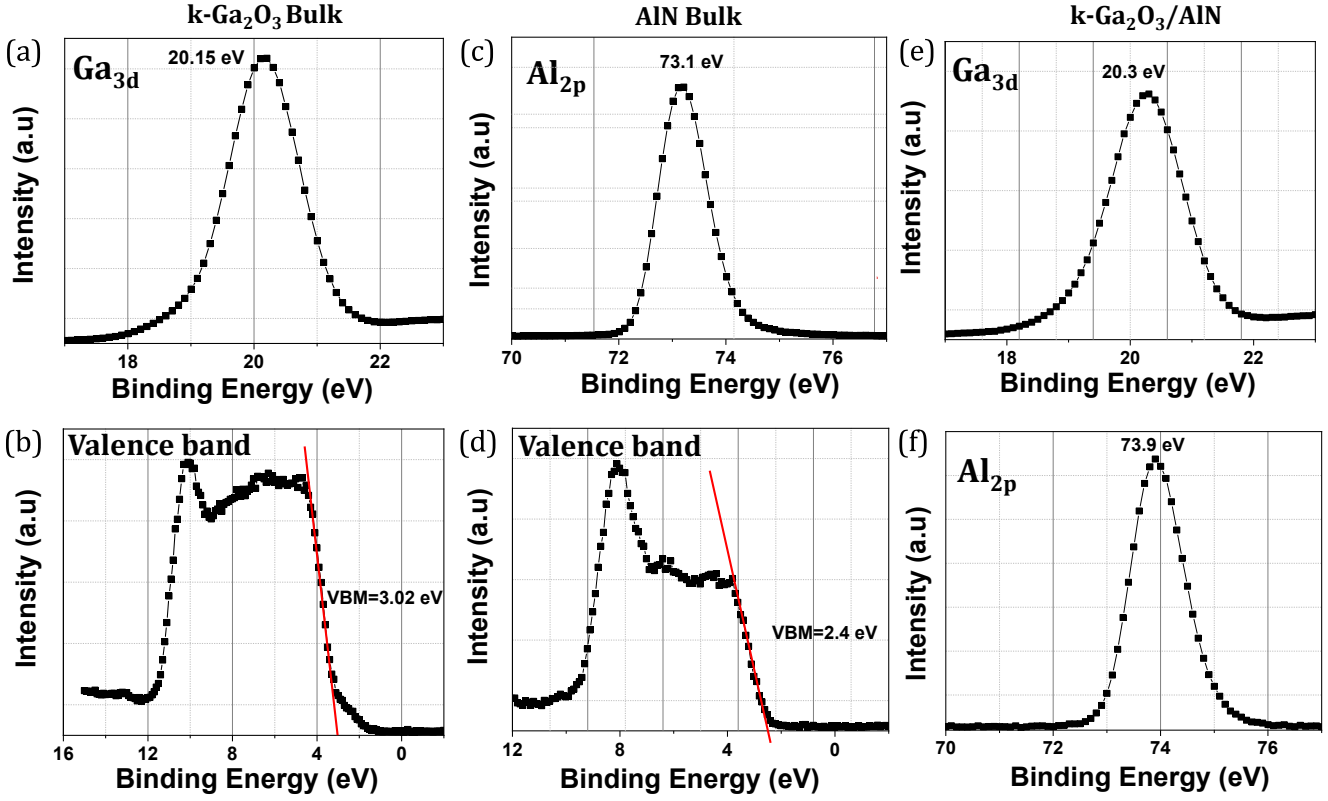

Fig. 4. XPS core level spectra of (a) Ga_{3d} and (b) valence band spectra of the κ-Ga_2O_3; core level spectra of (c) Al_{2p} and (d) valence band spectra of the AlN; core level spectra of (e) Ga_{3d} and (f) Al_{2p} of the κ-Ga_2O_3/AlN heterostructure.

Table 2
Fitting parameters used for VBO calculation of κ-Ga_2O_3/AlN.

Sample	State	Binding energy (eV)	Bonding	FWHM(eV)
κ-Ga_2O_3	Ga_{3d}	20.2	Ga-O	1.3
	VBM	3.02		
AlN	Al_{2p}	73.1	Al-N	0.37
	VBM	2.4		
κ-Ga_2O_3/AlN	Ga_{3d}	20.3	Ga-O	1.3
	Al_{2p}	73.9	Al-N	1.1

$$\Delta E_V = (E^{k-Ga2O3}_{Ga3d} - E^{k-Ga2O3}_{VBM}) - (E^{AlN}_{Al2p} - E^{AlN}_{VBM}) + (E^{k-Ga2O3/AlN}_{Ga3d} - E^{k-Ga2O3/AlN}_{Al2p}) \quad (3)$$

E_{Ga3d} and E_{Al2p} represent the peak binding energy position of the Ga_{3d} and Al_{2p} CL spectra, respectively, while E_{VBM} denotes the valence band maximum position. Fig. 4 (a) and 4 (b) represent the Ga_{3d} CL and valence band spectra of κ-Ga_2O_3 bulk film. In Fig. 4 (a), Ga_{3d} binding energy is positioned at 20.15 eV with a Gaussian peak FWHM value of 1.3 eV. The valance band maximum value was evaluated to be 3.02 eV from the valence band spectra (Fig. 4 (b)). From Fig. 4 (c) and 4 (d) (for bulk AlN film), Al_{2p} position and VBM values were calculated to be 73.1 eV and 2.4 eV, respectively. These values are in good agreement with our previous report [21]. Fig. 4(e) and 4(f) show the Ga_{3d} and Al_{2p} CLs, which originated from heterostructure, respectively. The details of the fitting parameters and binding energy positions are tabulated in Table 2. Putting all these experimental values in equation (3), the VBO for κ-Ga_2O_3/AlN heterostructure is determined to be 0.08 ± 0.07 eV.

The conduction band offset (ΔE_C) for κ-Ga_2O_3/AlN heterostructure is determined by substituting the VBO and the electronic bandgap values in the equation, $\Delta E_C = E_g^{k-Ga2O3} - E_g^{AlN} + \Delta E_V$. Thereby, CBO is calculated to be 1.04 ± 0.07 eV, where the E_g^{AlN} is measured to be 6.12 eV from the transmittance tauc plot (supplementary information S3).

Fig. 5 represents the band alignment of both κ-Ga_2O_3/GaN and κ-Ga_2O_3/AlN heterostructure, which forms a type-I band alignment. However, in our previous study, the monoclinic β-Ga_2O_3/AlN heterostructure forms a type-II band alignment with VBO of − 0.55 ± 0.05 eV [21]. While the monoclinic β-Ga_2O_3/GaN heterostructure forms a type-I band alignment with a high VBO of 1.4 ± 0.08 eV [27]. This particular difference in electronic band alignment property of the same material with different phases could be utilized for various applications. In the present study, the formation of type-I is interesting for developing high electron mobility transistors for two reasons. First of all, κ-Ga_2O_3 possesses spontaneous polarisation and ferroelectric properties so that the polarization can be tuned by applying bias voltage [19]; however other phases of Ga_2O_3 do not show this unique material property. Secondly, integrating well-established nitride polarization materials with ferroelectric κ-Ga_2O_3 will allow more space for tunability of the polarization difference between the materials and thereby carrier concentration within the interface. There are a few simulation studies which explain the huge interface charges at the κ-Ga_2O_3/(Al, Ga)N interface [15,17]. Moreover, the experimental results of the band alignment study suggest that the electron affinity of κ-Ga_2O_3 will be lesser than the electron affinity of β-Ga_2O_3 (χ = 3.15 eV).

4. Conclusions

In conclusion, orthorhombic Ga_2O_3 was deposited on GaN and AlN templates to form a heterojunction. XPS measurements were carried out to determine the VBO and CBO of κ-Ga_2O_3/GaN and κ-Ga_2O_3/AlN heterostructures. κ-Ga_2O_3 forms a type-I heterojunction with GaN and AlN with high CBO values of 1.38 ± 0.07 eV and 1.04 ± 0.07 eV, respectively. The existence of spontaneous polarisation property along with unique band alignment suggests the possibility of 2DCG at the heterointerface. Therefore, this work could lead to the development of efficient power devices with tunable carrier concentrations.

CRediT authorship contribution statement

Shibin Krishna: Conceptualization, Investigation, Methodology, Data curation, Formal analysis, Writing – original draft, Writing – review & editing. **Yi Lu:** Methodology. **Che-Hao Liao:** Methodology. **Vishal Khandelwal:** . **Xiaohang Li:** Conceptualization, Investigation, Funding acquisition, Project administration, Resources, Supervision, Validation, Writing – review & editing.

Declaration of Competing Interest

The authors declare that they have no known competing financial interests or personal relationships that could have appeared to influence the work reported in this paper.

Acknowledgment

The authors would like to acknowledge the support of KAUST Baseline BAS/1/1664-01-01. We thank Qingxiao Wang for performing the STEM measurements and for helpful discussions.

Appendix A. Supplementary material

Supplementary data to this article can be found online at https://doi.org/10.1016/j.apsusc.2022.153901.

References

[1] C.G. Van de Walle, J. Neugebauer, Universal alignment of hydrogen levels in semiconductors, insulators and solutions, Nature 423 (2003) 626–628.
[2] S. Juneja, R. Pratap, R. Sharma, Semiconductor technologies for 5G implementation at millimeter wave frequencies – Design challenges and current state of work, Engineering Science and Technology, an, International Journal 24 (2021) 205–217.
[3] T. Ueda, GaN power devices: current status and future challenges, Jpn. J. Appl. Phys. 58 (SC) (2019) SC0804, https://doi.org/10.7567/1347-4065/ab12c9.
[4] D. Guo, Q. Guo, Z. Chen, Z. Wu, P. Li, W. Tang, Review of Ga2O3-based optoelectronic devices, Materials Today Physics 11 (2019) 100157, https://doi.org/10.1016/j.mtphys.2019.100157.
[5] S.J. Pearton, J. Yang, P.H. Cary, F. Ren, J. Kim, M.J. Tadjer, M.A. Mastro, A review of Ga2O3 materials, processing, and devices, Appl. Phys. Rev. 5 (2018), 011301.
[6] H. von Wenckstern, Group-III Sesquioxides: Growth Physical Properties and Devices, Adv. Electron. Mater. 3 (9) (2017) 1600350, https://doi.org/10.1002/aelm.v3.910.1002/aelm.201600350.
[7] X. Tang, K.-H. Li, C.-H. Liao, D. Zheng, C. Liu, R. Lin, N.a. Xiao, S. Krishna, J. Tauboada, X. Li, Epitaxial growth of β-Ga2O3 (−201) thin film on four-fold symmetry CeO2 (001) substrate for heterogeneous integrations, J. Mater. Chem. C 9 (44) (2021) 15868–15876.
[8] X. Yang, X. Du, L. He, D.i. Wang, C. Zhao, J. Liu, J. Ma, H. Xiao, Fabrication and optoelectronic properties of Ga2O3/Eu epitaxial films on nanoporous GaN distributed Bragg reflectors, J. Mater. Sci. 55 (19) (2020) 8231–8240.
[9] X. Yang, X. Du, J. Liu, R. Chen, D.i. Wang, Y. Le, H. Zhu, B.o. Feng, J. Ma, H. Xiao, Effects of porosity on the structural and optoelectronic properties of Er-doped Ga2O3 epitaxial films on etched epi-GaN/sapphire substrates, Ceram. Int. 47 (7) (2021) 9597–9605.
[10] B.R. Tak, S. Kumar, A.K. Kapoor, D. Wang, X. Li, H. Sun, R. Singh, Recent advances in the growth of gallium oxide thin films employing various growth techniques—a review, J. Phys. D Appl. Phys. 54 (45) (2021) 453002, https://doi.org/10.1088/1361-6463/ac1af2.
[11] R. Batra, H.D. Tran, B. Johnson, B. Zoellner, P.A. Maggard, J.L. Jones, G. A. Rossetti, R. Ramprasad, Search for Ferroelectric Binary Oxides: Chemical and Structural Space Exploration Guided by Group Theory and Computations, Chem. Mater. 32 (2020) 3823–3832.
[12] J. Kim, D. Tahara, Y. Miura, B.G. Kim, First-principle calculations of electronic structures and polar properties of (κ, ε)-Ga2O3, Appl. Phys Express 11 (2018), 061101.
[13] J. Lee, H. Kim, L. Gautam, M. Razeghi, High Thermal Stability of κ-Ga2O3 Grown by MOCVD, Crystals 11 (4) (2021) 446, https://doi.org/10.3390/cryst11040446.
[14] K. Shimada, First-principles study of crystal structure, elastic stiffness constants, piezoelectric constants, and spontaneous polarization of orthorhombicPna21-M2O3(M = Al, Ga, In, Sc, Y), Mater. Res. Express 5 (2018), 036502.
[15] M.B. Maccioni, V. Fiorentini, Phase diagram and polarization of stable phases of (Ga1−xInx)2O3, Appl. Phys Express 9 (2016), 041102.
[16] K. Liu, H. Sun, F. AlQatari, W. Guo, X. Liu, J. Li, C.G. Torres Castanedo, X. Li, Wurtzite BAlN and BGaN alloys for heterointerface polarization engineering, Appl. Phys. Lett. 111 (22) (2017) 222106, https://doi.org/10.1063/1.5008451.

[17] S. Leone, R. Fornari, M. Bosi, V. Montedoro, L. Kirste, P. Doering, F. Benkhelifa, M. Prescher, C. Manz, V. Polyakov, O. Ambacher, Epitaxial growth of GaN/Ga2O3 and Ga2O3/GaN heterostructures for novel high electron mobility transistors, J. Cryst. Growth 534 (2020) 125511, https://doi.org/10.1016/j.jcrysgro.2020.125511.
[18] X. Xia, H. Liang, X. Geng, Y. Chen, C. Yang, Y. Liu, R. Shen, M. Xu, G. Du, Synthesis of GaN network by nitridation of hexagonal ε-Ga2O3 film, J. Mater. Sci.: Mater. Electron. 28 (3) (2017) 2598–2601.
[19] F. Mezzadri, G. Calestani, F. Boschi, D. Delmonte, M. Bosi, R. Fornari, Crystal Structure and Ferroelectric Properties of ε-Ga2O3 Films Grown on (0001)-Sapphire, Inorg. Chem. 55 (22) (2016) 12079–12084.
[20] S.K. Tc, G. Gupta, Band alignment and Schottky behaviour of InN/GaN heterostructure grown by low-temperature low-energy nitrogen ion bombardment, RSC Adv. 4 (52) (2014) 27308–27314.
[21] H. Sun, C.G. Torres Castanedo, K. Liu, K.-H. Li, W. Guo, R. Lin, X. Liu, J. Li, X. Li, Valence and conduction band offsets of β-Ga2O3/AlN heterojunction, Appl. Phys. Lett. 111 (2017), 162105.
[22] M. Kneiß, A. Hassa, D. Splith, C. Sturm, H. von Wenckstern, T. Schultz, N. Koch, M. Lorenz, M. Grundmann, Tin-assisted heteroepitaxial PLD-growth of κ-Ga2O3 thin films with high crystalline quality, APL Mater. 7 (2018), 022516.
[23] M. Kracht, A. Karg, J. Schörmann, M. Weinhold, D. Zink, F. Michel, M. Rohnke, M. Schowalter, B. Gerken, A. Rosenauer, P.J. Klar, J. Janek, M. Eickhoff, Tin-Assisted Synthesis of e-Ga2O3 by Molecular Beam Epitaxy, Phys. Rev. Appl 8 (2017), 054002.
[24] K. Matsuzaki, H. Yanagi, T. Kamiya, H. Hiramatsu, K. Nomura, M. Hirano, H. Hosono, Field-induced current modulation in epitaxial film of deep-ultraviolet transparent oxide semiconductor Ga2O3, Appl. Phys. Lett. 88 (2006), 092106.
[25] K. Jiang, J. Tang, M.J. Cabral, A. Park, L. Gu, R.F. Davis, L.M. Porter, Layered phase composition and microstructure of κ-Ga2O3-dominant heteroepitaxial films grown via MOCVD, J. Appl. Phys. 131 (2022), 055305.
[26] I. Cora, F. Mezzadri, F. Boschi, M. Bosi, M. Čaplovičová, G. Calestani, I. Dódony, B. Pécz, R. Fornari, The real structure of ε-Ga2O3 and its relation to κ-phase, CrystEngComm 19 (2017) 1509–1516.
[27] W. Wei, Z. Qin, S. Fan, Z. Li, K. Shi, Q. Zhu, G. Zhang, Valence band offset of β-Ga2O3/wurtzite GaN heterostructure measured by X-ray photoelectron spectroscopy, Nanoscale Res. Lett. 7 (2012) 562.